Model-Based Selection of Accelerometer Locations for Helicopter Gearbox Monitoring

Keming Wang
Visiting Scholar

Dongzhe Yang
Graduate Research Assistant

Kourosh Danai
Professor[1]

David G. Lewicki
Vehicle Technology Center
U.S. Army Research Laboratory
NASA Glenn Research Center
Cleveland, Ohio

Department of Mechanical and Industrial Engineering
University of Massachusetts, Amherst, Massachusetts

A novel method is introduced to quantify, based on the structure of the gearbox, the monitoring effectiveness of accelerometer locations on the housing. In this method, *monitoring effectiveness* of sets of accelerometer locations is defined in terms of two indices: the *coverage index* and the *overlap index*. The coverage index is obtained from an influence matrix defining the level of effect of component faults on accelerometer readings. The overlap index denotes the level of overlap between pairs of accelerometers in coverage of components. The effectiveness of the proposed method is verified experimentally based on measurement-fault data obtained from an OH-58A main rotor gearbox. The estimated rankings of various sets of accelerometer locations based on the estimated values of their monitoring effectiveness agree closely with those obtained empirically.

Introduction

Helicopter gearboxes are major causes of flight safety incidents. For example, a U.S. Army study indicates that power plants and transmission systems have contributed to 68% of flight safety incidents related to failure in mechanical systems and to 58% of direct maintenance costs (Ref. 1). Effective and reliable condition monitoring and fault diagnosis of helicopter gearboxes enhances personnel safety by preventing catastrophic breakdowns, and reduces repair costs by improving maintenance strategy (Ref. 2).

Among the various approaches to helicopter gearbox fault diagnosis (e.g., debris and acoustic monitoring), vibration monitoring is the most investigated and widely used approach. In this approach, the vibration signals are measured by accelerometers mounted on the housing and analyzed on-line for fault detection and isolation. Given that different housing locations receive different responses to component faults, one needs to determine where to mount the accelerometers and how many to use in order to cover all the components in the gearbox.

Accelerometers are generally located by experts based on their proximity to gearbox components, orientation, and ease of mounting on the housing. Although this approach is practical, it often leads to too many accelerometers for the on-board computer to monitor while demanding excessive numbers of mounting, cabling, and signal conditioning equipment. As such, experts are often faced with the dilemma as which accelerometer(s) to eliminate without seriously undermining coverage of the gearbox components. This dilemma can of course be solved empirically, but given that comprehensive sets of vibration data are often not available for gearboxes, accelerometer locations are usually selected by intuition.

Manuscript received January 1998; accepted May 1999.

[1]To whom all correspondence should be addressed

In this paper, a model-based method is presented to quantify the effectiveness in monitoring of various combinations of accelerometers. This method is based on (1) a structural influence matrix which represents qualitatively the proximity effect of individual component faults on accelerometer readings, and (2) an overlap matrix which defines the mutual overlap between pairs of accelerometers in their coverage of various gearbox components. Based on these matrices, indices are defined to characterize the coverage of components by accelerometers and the overlap of accelerometers with each other. Using these indices, the *monitoring effectiveness* of various combinations of accelerometer locations can be computed. The performance of this method is evaluated in application to an OH- 58A helicopter main rotor gearbox for which vibration data is available at several fault instances. Results indicate that the theoretical rankings obtained for various accelerometer suites are in close agreement with empirically obtained rankings. This indicates that the proposed selection method can be reliably used for evaluation of candidate accelerometer locations and their optimal selection.

Selection Method

Good mounting locations for accelerometers on the housing are generally those that provide both good proximity to gearbox components and ease of mounting. However, considering that only a limited number of accelerometers can by used, those candidate locations need to be selected that provide a comprehensive coverage of the components. The method presented here for accelerometer location selection follows this same principle. In this method, the coverage offered by each candidate location is represented by a *coverage index*, and its overlap with other candidate locations in coverage of the gearbox components is denoted by an *overlap index*. The monitoring effectiveness of various combinations of accelerometer locations is then estimated as a function of the coverage and overlap indices of the accelerometer locations.

Coverage index

The coverage index denotes the reach of each accelerometer in covering various components of the gearbox. It is computed based on a structural influence matrix defined to represent the proximity effect of various component faults on accelerometer readings. Ideally, the influence coefficient between a component and an accelerometer should be defined such that it would represent the strength of vibration registered by the accelerometer as a result of a fault in the component. However, the strength of vibration depends on the attenuation property of the transfer path between the component and the accelerometer and is a function of parameters such as the moment of inertia, stiffness, and damping of the components in the path (Refs. 3, 4), which cannot be accurately quantified. For example, the gear mesh stiffness is obtained by considering the gear tooth as a non-uniform cantilever beam (Refs. 5, 6), as a function of the cross-section of the tooth at the point of loading as well as load variation due to changes in direction of load application (Refs. 5, 7, 8), friction between the meshing teeth (Ref. 9), contact ratio (Ref. 10), the type of gears (spur, helical, etc.) (Refs. 5, 6, 8), and gear errors such as profile, transmission, and manufacturing errors (Refs. 4, 8). Similarly, the stiffness of bearings is a time-varying, non-linear function of bearing displacement and the number of rolling elements in the load zone, as well as the bearing type (roller, ball, etc.), axial preload, clearance, and race waviness (Refs. 11–13).

In view of the difficulties associated with precise modeling of vibration, a simplified method is devised here that accounts separately for the two main aspects of vibration change due to faulty components: (1) the proximity effect of the faulty component on the accelerometer generating the feature (structural influence), and (2) the frequency represented by the feature (featural influence). Structural influences in this research are defined to represent the average strength of the vibration signal across all frequencies measured by an accelerometer due to a component fault (Refs. 14, 15). This average vibration is computed through the following simplifications: (1) a lumped-mass model of the gearbox is employed to represent its structure; (2) in the absence of accurate values for stiffness coefficients, only the average static values for the stiffness coefficients are used; (3) damping ratios of bearings and shafts are neglected (Ref. 5); (4) the damping ratio of gears estimated between 0.03 and 0.17 (Ref. 16) is set at 0.1 for all gears; (5) the cross-coupling terms in the stiffness matrix are neglected; (6) those vibration travel paths that are much longer than the shortest one between component-accelerometer pairs are neglected; and (7) vibration transfer through the housing is considered only when a housing path is shorter and more direct than the component paths.

Using the above simplifications, the average vibration registered by an accelerometer due to a faulty component can be simulated by applying an excitation source at the component in the lumped-mass model (see Fig. 1). Furthermore, in order to represent all frequencies in the excitation source, the excitation can be selected to consist of unit amplitude sine waves of all frequencies. The displacement of various components in the travel path due to an excitation exerted at the ith component can be obtained for a typical N-mass path as (Ref. 17):

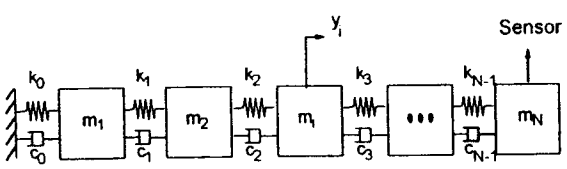

Fig. 1. Illustration of the lumped mass model of the gearbox components.

$$\begin{bmatrix} a_{11} & a_{12} & 0 & \cdots & 0 \\ a_{21} & a_{22} & a_{23} & \cdots & 0 \\ \vdots & \vdots & \vdots & \cdots & \vdots \\ 0 & \cdots & 0 & a_{NN-1} & a_{NN} \end{bmatrix} \begin{bmatrix} x_1 \\ x_2 \\ \vdots \\ x_N \end{bmatrix} = \begin{bmatrix} 0 \\ 0 \\ y_i \\ 0 \end{bmatrix} \tag{1}$$

where $[x_1, x_2, \ldots, x_N]^T$ represent the displacements of the N components in the path, y_i denotes the magnitude of excitation at the ith component, and the coefficients a_{ii}, a_{ii-1}, and a_{ii+1} are defined as:

$$\begin{aligned} a_{ii-1} &= -jwc_{i-1} - k_{i-1} \\ a_{ii} &= -m_i w^2 + jw(c_{i-1} + c_i) + (k_{i-1} + k_i) \\ a_{ii+1} &= -jwc_i - k_i. \end{aligned} \tag{2}$$

In the above equation, m_i denotes the mass of the ith component, k_i and c_i represent the stiffness and damping coefficients between the ith and $(i+1)$th components, respectively, and w denotes frequency. This computation is based on the assumption that each vibration travel path starts from a fixed point within the gearbox, and the vibration caused by the faulty component travels through all of the components in the path and terminates at the casing. Given that there are actually no fixed points in a gearbox, this is another simplification used to facilitate the computation of average vibration values.

In this research, to represent the overall vibration transferred from the component to the accelerometer, the average vibration from the component is characterized by the root mean square (RMS) value of vibration across all frequencies (Ref. 14). RMS values of vibration are readily obtained from Eq. (1) by numerical integration of the square of displacements across all frequencies. In these calculations, to avoid unnecessary numerical problems at the natural frequencies of the components with negligible damping, the integration is carried out by excluding the natural frequencies.

For the purpose of assigning structural influence coefficients, the RMS values are scaled so that the component directly adjacent to the accelerometer has the highest influence coefficient. Different functions can be used for defining influence coefficients. Here, the influence coefficients are defined as:

$$I_i = \frac{\log(r_i)}{\log(r_N)} \tag{3}$$

where r_i represents the RMS value of vibration with the excitation source at the ith component, and r_N denotes the RMS value of vibration when the excitation is at the Nth component. In both cases, the accelerometer is considered at the Nth component. The influence coefficient for the other components is obtained in a similar fashion by moving the excitation source to them in the travel path.

The simplifications used to facilitate the calculation of vibration result in only approximate influence coefficient values. In order to cope with the approximate nature of the influence coefficients, they are defined in terms of fuzzy variables (Ref. 18), so they are not treated as precise values but as variables with a range. The influence coefficient values from Eq. (3) are transformed into the following fuzzy variables: Nil: (0, 0.1), Low: (0.1, 0.4), Medium: (0.4, 0.6), High: (0.6, 0.9) and Definite: (0.9, 1), so as to define the fuzzy influence coefficients in the influence model (Ref. 14).

Based on the above fuzzy influence coefficients, the coverage index is defined as the sum of the individual rows of the influence matrix, as:

$$C_j = \frac{1}{N} \sum_{i=1}^{N} \frac{u_{ij} + l_{ij}}{2} \tag{4}$$

where u_{ij} and l_{ij} represent the upper and lower limits of the fuzzy influence coefficients between the gearbox component i and accelerometer j,

and N denotes the total number of gearbox components. The coverage index represents the coverage of all the components within the gearbox by an accelerometer. Since the coverage index is a measure of an accelerometer's reach of the gearbox components, an accelerometer location with a higher coverage index is a better candidate. As such, the coverage index should be a factor in estimating the monitoring effectiveness of sets of accelerometer locations.

Overlap index

The coverage index can be used to rank accelerometers individually. However, for a complex gearbox where more than one accelerometer is needed for monitoring, the sum of the coverage indices associated with all of the accelerometers in the suite would not provide a correct representation of their overall effectiveness, because it would ignore the overlap among them.

The overlap between accelerometer pairs may be defined according to the influence coefficients. But that definition would only consider the distance of the accelerometers from the components, and would ignore factors such as accelerometer orientation and gearbox size. In order to consider these other factors, the overlap index is defined independent of the influence coefficients, based on an overlap matrix that represents the level of co-coverage between all of the accelerometer pairs. The individual components O_{jk} in this matrix are defined as:

$$O_{jk} = \frac{E_{jk}}{e^{aD_{jk}}}(1 + S_{jk}) \tag{5}$$

where O_{jk} denotes the overlap between accelerometers j and k, E_{jk} represents the similarity of orientation between the two accelerometers, a is a constant to account for the size of the gearbox, D_{jk} accounts for the physical distance between the two accelerometers, and S_{jk} is a symmetry factor between the two accelerometers. The formulation of Eq. (5) is based on the following analogy: The overlap in coverage of two accelerometers depends mainly on their orientation and location, that is, the more identical their orientation is and the closer they are mounted to each other, the higher is their expected level of overlap. In the above equation, the orientation factor $E_{jk} \in [0, 1]$ is set to 1 when accelerometers j and k have identical orientation. The distance factor $D_{jk} \in [0, 1]$ is defined as the normalized shortest geometrical distance between the two accelerometers along the casing, where the term $e^{aD_{jk}}$ approximates the attenuation of vibration due to distance (Ref. 19) and the constant a, with values ranging between 0 and 2, accounts for the effect of gearbox size on vibration attenuation. Although the main factors in the coverage overlap of two accelerometers are orientation and distance, the accelerometers that are symmetrically positioned are believed to have a larger overlap with each other. In order to account for this factor, a symmetry factor $S_{jk} \in [0, 1]$ is also included in Eq. (5) which is set to 1 when two accelerometers are exactly symmetric with respect to the housing. Based on Eq. (5), the values of O_{jk} would ordinarily fall in the range [0, 1], where the value of 1 indicates that the two accelerometers j and k have 100% overlap with each other and that one of them can be removed. Similarly, when O_{jk} is determined as 0 then the two accelerometers are assumed to be covering completely different components. It should, of course, be noted that some overlap between accelerometers is considered useful, and is often factored in the selection of accelerometer locations.

The overlap coefficients only represent the level of overlap between pairs of accelerometers and not the specific components covered jointly by each accelerometer pair. As such, defining the level of overlap between several accelerometers is not as straightforward. At one extreme, one can assume that the coverage overlap of each accelerometer pair in the suite does not coincide with the coverage overlap of the other accelerometer pairs, so the total overlap O_s for the accelerometer suite can be computed as

$$O_s = \sum_{j=1}^{m} Min\left(\sum_{k=j+1}^{m} O_{jk} \frac{C_j + C_k}{2}, C_j \right) \tag{6}$$

where m denotes the number of accelerometers in the suite, and the *Min* function ensures that the computed overlap will not exceed the total coverage of accelerometer j. At the other extreme, it can be assumed that the overlap of all of the accelerometer pairs coincide, and that the total overlap of the accelerometer suite can be defined as

$$O_s = \sum_{j=1}^{m} Max\left(O_{jk} \frac{C_j + C_k}{2} \text{ for all } k > j \right) \tag{7}$$

which only considers the largest overlap between accelerometer j and the other accelerometers in the suite. It is also possible to use the average of the above two extremes as a compromise:

$$O_s = \sum_{j=1}^{m} \frac{1}{2} \left[\left(Min\left(\sum_{k=j+1}^{m} O_{jk} \frac{C_j + C_k}{2}, C_j \right) \right) + \left(Max\left(O_{jk} \frac{C_j + C_k}{2} \text{ for all } k > j \right) \right) \right] \tag{8}$$

It should be noted that, unlike the coverage index, the overlap index is suite-related because the overlap of an accelerometer depends on the other accelerometers in the suite.

Monitoring effectiveness

As mentioned earlier, the coverage index can be used to evaluate the effectiveness of individual accelerometers in monitoring, but its sum cannot be used to evaluate suites of accelerometers. For instance, a suite consisting of the top three accelerometer locations coverage-wise may be inferior to another suite of three accelerometer locations with a lower total level of coverage but less overlap among the accelerometers. The best set of accelerometer locations is one which provides the highest coverage of the gearbox components and the least overlap among the accelerometers. As such, the monitoring effectiveness ME of a suite can be expressed as:

$$ME_s = \left(\sum_{j=1}^{m} C_j \right) - O_s \tag{9}$$

where m represents the number of accelerometers in the suite, C_i denotes the coverage of individual accelerometers in the suite and O_s represents the total overlap among the accelerometers in the suite, estimated from any one of Eqs. (6)–(8).

Experimental

The validity of the proposed accelerometer location method was tested in application to an OH-58A main rotor gearbox, where the vibration data collected during normal conditions and at fault instances were used to obtain empirical rankings for various accelerometer suites. Experimental vibration data for the OH-58A gearbox were collected at the NASA Lewis Research Center as part of a joint NASA/Navy/Army advanced lubricants program (Ref. 20). Various component failures in the OH-58A transmission were produced during accelerated fatigue tests. The vibration signals were recorded by eight piezoelectric accelerometers (frequency range of up to 10 KHz) using an FM tape recorder. The signals were recorded once

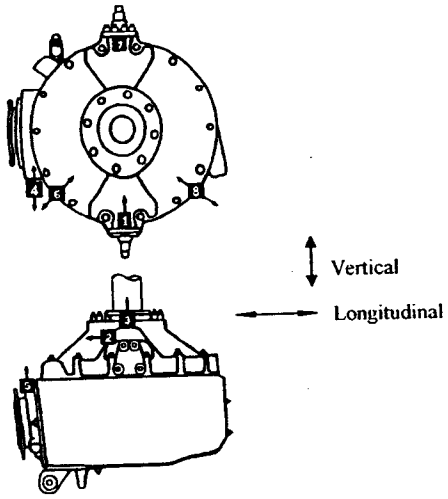

Fig. 2. Location of accelerometers on the test stand.

every hour, for about one to two minutes per recording (using a bandwidth of 20 KHz). Two magnetic chip detectors were also used to detect the debris caused by component failures. The location and orientation of the accelerometers are shown in Fig. 2. The OH-58A gearbox was run under a constant load and was disassembled and inspected periodically, or when one of the chip detectors indicated a failure. A total of eleven failures occurred during these tests. They consisted of three cases of planet bearing pitting fatigue, three cases of sun gear pitting fatigue, two cases of top housing cover cracking, and one case each of spiral bevel pinion pitting fatigue, mast bearing micropitting, and planet gear pitting fatigue.

Application of the Method

The application of the proposed method to the OH-58A main rotor transmission (see Fig. 3) would require definition of the influence matrix for this gearbox. To derive the influence coefficients, six vibration travel paths were defined as follows: (1) fixed point-Duplex Bearing and[2] Gear Roller Bearing-Spiral Bevel Gear-Spiral Bevel Pinion-Triplex Bearing, (2) fixed point-Pinion Roller Bearing-Pinion Shaft-Triplex Bearing, (3) fixed point-Duplex Bearing-Sun Planet mesh-Ring Gear, (4) fixed point-Mast Roller Bearing and Main Shaft Ball Bearing-Main Shaft-Planet Bearing-Planet Gear-Ring Gear, (5) fixed point-Main Shaft Ball Bearing-Ring Gear through Casing, (6) fixed point-Gear Roller Bearing-Ring Gear through Casing. The first two travel paths were in connection to Accelerometers 4, 5, and 6, whereas all the other paths were connected to Accelerometers 1, 2, 3, 6, 7, and 8. Note that every path started from a bearing within the gearbox and ended at a component close to a candidate accelerometer location on the Casing. For computation of the influence coefficients, the end lumped-mass of every path was the Casing where an accelerometer was mounted.

Considering that due to fuzzification of influence coefficients, adjacent components with potentially the same fuzzy influence coefficients may become indistinguishable for ranking purposes, the OH-58A gearbox was divided into three subsystems (see Fig. 3): Subsystem 1 (the Input Subsystem), Subsystem 2 (the Output Subsystem), and Subsystem 3 (the Planetary Subsystem). Table 1 shows the distribution of the gearbox components among the subsystems, along with with the fuzzy influence coefficients obtained for all of the accelerometer-component pairs.

[2]and means parallel

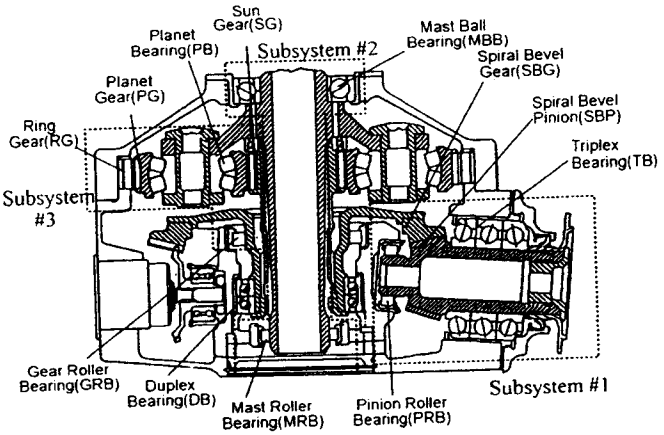

Fig. 3. Layout of the various components in the OH-58A gearbox. The figure also shows division of the gearbox into subsystems for diagnostic purposes.

The influence coefficients between the subsystems and accelerometers were obtained by averaging the component influence coefficients within each subsystem. The lower and upper values of the influence coefficients for these three subsystems are shown in Table 2.

The eight candidate accelerometer locations (see Fig. 2 for their locations and orientations), which were actually used for vibration measurement during accelerated fatigue tests of the gearbox, were analyzed and ranked for their significance in monitoring. In order to obtain the overlap coefficients for the OH-58A gearbox, the values of the orientation factors E_{ik}, distance factors D_{ik}, and symmetry factors S_{ik} for the eight accelerometer locations were defined as:

$$E_{jk} = \begin{bmatrix} 1 & 0.5 & 0.3 & 1 & 0.4 & 0.8 & 1 & 0.8 \\ 0.5 & 1 & 0.3 & 0.5 & 0.4 & 0.7 & 0.5 & 0.7 \\ 0.3 & 0.3 & 1 & 0.4 & 1 & 0.3 & 0.3 & 0.3 \\ 1 & 0.5 & 0.4 & 1 & 0.4 & 0.5 & 1 & 0.8 \\ 0.4 & 0.4 & 1 & 0.4 & 1 & 0.4 & 0.4 & 0.4 \\ 0.8 & 0.7 & 0.3 & 0.5 & 0.4 & 1 & 0.8 & 0.6 \\ 1 & 0.5 & 0.3 & 1 & 0.4 & 0.8 & 1 & 0.8 \\ 0.8 & 0.7 & 0.3 & 0.8 & 0.4 & 0.6 & 0.8 & 1 \end{bmatrix}$$

$$aD_{jk} = \begin{bmatrix} 0 & 0 & 0 & 1.5 & 1.5 & 0.5 & 2.0 & 0.5 \\ 0 & 0 & 0 & 1.5 & 1.5 & 0.5 & 2.0 & 0.5 \\ 0 & 0 & 0 & 1.5 & 1.5 & 0.5 & 2.0 & 0.5 \\ 1.5 & 1.5 & 1.5 & 0 & 0.8 & 1.0 & 1.5 & 2.0 \\ 1.5 & 1.5 & 1.5 & 0.8 & 0 & 1.0 & 1.5 & 2.0 \\ 0.5 & 0.5 & 0.5 & 1.0 & 1.0 & 0 & 1.5 & 1.0 \\ 2.0 & 2.0 & 2.0 & 1.5 & 1.5 & 1.5 & 0 & 1.5 \\ 0.5 & 0.5 & 0.5 & 2.0 & 2.0 & 1.0 & 1.5 & 0 \end{bmatrix}$$

$$S_{jk} = \begin{bmatrix} 0 & 0 & 0 & 0 & 0 & 0 & 1 & 0 \\ 0 & 0 & 0 & 0 & 0 & 0 & 1 & 0 \\ 0 & 0 & 0 & 0 & 0 & 0 & 1 & 0 \\ 0 & 0 & 0 & 0 & 0 & 0 & 1 & 0 \\ 0 & 0 & 0 & 0 & 0 & 0 & 0 & 0 \\ 0 & 0 & 0 & 0 & 0 & 0 & 0 & 1 \\ 1 & 1 & 1 & 1 & 0 & 0 & 0 & 0.5 \\ 0 & 0 & 0 & 0 & 0 & 1 & 0.5 & 0 \end{bmatrix}$$

Using the above values, the overlap coefficients for the eight locations were determined from Eq. (5) as

Table 1. Distribution of gearbox components within the subsystems

Gearbox Component	Abbreviation	Subsystem	Accelerometer 1	2	3	4	5	6	7	8
Triplex Bearing	TB	1	-	-	-	H	H	H	-	-
Spiral Bevel Pinion	SBP	1	-	-	-	H	H	M	-	-
Pinion Roller Bearing	PRB	1	-	-	-	M	M	L	-	-
Spiral Bevel Gear	SBG	1	-	-	-	M	M	L	-	-
Duplex Bearing	DB	1	M	M	M	M	M	L	M	M
Mast Roller Bearing	MRB	2	M	M	M	-	-	M	M	M
Main Shaft	MS	2	M	M	M	-	-	M	M	M
Mast Ball Bearing	MBB	2	M	M	M	-	-	M	M	M
Sun Gear	SG	3	M	M	M	M	M	M	M	M
Planet Bearing	PB	3	H	H	H	H	H	M	H	H
Planet Gear	PG	3	H	H	H	M	M	M	H	H
Ring Gear	RG	3	H	H	H	H	H	M	H	H
Gear Roller Bearing	GRB	3	H	H	H	H	H	H	H	H

Table 2. The lower and upper value of the three subsystem influence coefficients on the eight accelerometers

Accelerometer	Subsystems: Input		Output		Planetary	
1	0.008	0.158	0.233	0.467	0.650	0.950
2	0.000	0.100	0.536	0.663	0.576	0.850
3	0.000	0.100	0.237	0.463	0.650	0.850
4	0.453	0.750	0.000	0.100	0.420	0.640
5	0.753	0.950	0.000	0.100	0.620	0.780
6	0.123	0.340	0.230	0.460	0.470	0.730
7	0.008	0.158	0.233	0.467	0.550	0.950
8	0.008	0.158	0.433	0.667	0.550	0.750

$$O_{jk} = \begin{bmatrix} 1 & 0.50 & 0.3 & 0.2 & 0.089 & 0.485 & 0.271 & 0.485 \\ 0.500 & 1 & 0.3 & 0.112 & 0.089 & 0.425 & 0.135 & 0.425 \\ 0.300 & 0.300 & 1 & 0.089 & 0.223 & 0.182 & 0.081 & 0.182 \\ 0.223 & 0.112 & 0.089 & 1 & 0.180 & 0.184 & 0.446 & 0.108 \\ 0.089 & 0.089 & 0.223 & 0.180 & 1 & 0.147 & 0.089 & 0.054 \\ 0.485 & 0.425 & 0.182 & 0.184 & 0.147 & 1 & 0.179 & 0.441 \\ 0.271 & 0.135 & 0.081 & 0.446 & 0.089 & 0.179 & 1 & 0.268 \\ 0.485 & 0.425 & 0.182 & 0.108 & 0.054 & 0.441 & 0.268 & 1 \end{bmatrix} \quad (10)$$

Given the above values of coverage and overlap, the monitoring effectiveness (ME) values were determined from Eq. (8) for various suites from the eight candidate accelerometer locations of the OH-58A main rotor gearbox. The ME values can be used, for example, to select the best set of accelerometer locations given a number of accelerometers to be used. A sample set of accelerometer locations with the highest and lowest rankings (from the 254 possible suites of the eight OH-58A locations) are shown in Table 3. Note that for some suite sizes several combinations of accelerometer locations are selected as 'best' and 'worst' suites, because in these cases the ME values were too close to render a suite better or worse than the other(s).

The ME values can also be used to assess the benefit of additional accelerometers, leading to larger suite sizes. To demonstrate this utility of monitoring effectiveness, the maximum ME value for each suite size was obtained (see Fig. 4). While additional accelerometers are expected to add to monitoring effectiveness, the added coverage they provide will diminish for larger suite sizes due to the increase in overlap between the accelerometers. This is clearly reflected in Fig. 4 where the mazimum ME value of the eight-strong accelerometer suite is the same as that of the

Table 3. Best and worst accelerometer suites within each suite size

Suite Size	Best Suite(s)	Worst Suite(s)
1 accelerometer	5	3
2 accelerometers	(5,8); (2,5)	(4,7); (1,6)
3 accelerometers	(2,5,7); (4,5,8); (2,4,5)	(1,6,8); (1,2,6); (1,2,8)
4 accelerometers	(3,4,5,8); (2,4,5,8); (2,4,5,7)	(1,2,7,8); (1,4,7,8); (1,6,7,8)
5 accelerometers	(2,3,4,5,8); (2,3,5,7,8); (2,3,5,6,7)	(1,4,6,7,8); (1,2,6,7,8); (1,2,4,7,8)
6 accelerometers	(1,2,3,4,5,7); (2,3,4,5,6,8)	(1,2,4,6,7,8); (1,3,4,6,7,8)
7 accelerometers	(1,2,3,4,5,6,8)	(1,2,3,4,6,7,8)

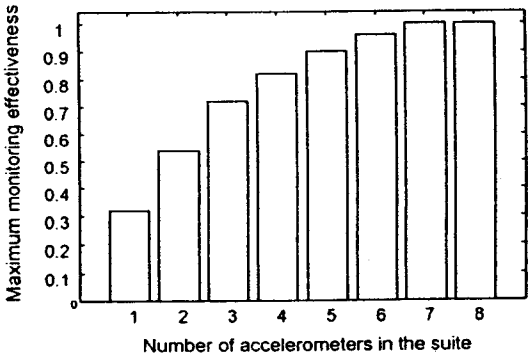

Fig. 4. Maximum values of monitoring effectiveness for different accelerometer suite sizes.

seven-strong accelerometer suite, and that the suite with 5 accelerometers has a maximum ME value of 0.90, only 10% less than that of the suite with 8 accelerometers.

Validation

The validity of the ME values was evaluated by comparing the rankings they provided for various accelerometer suites to the rankings obtained empirically from a series of diagnostic tests. The suites were ranked into four evenly spaced categories. The suites with the highest monitoring effectiveness were ranked as 1, and those with the lowest values were ranked into the 4th category. To obtain empirical rankings, a model-based diagnostic system was utilized which used as inputs the vibration features obtained from processing the vibration signals of individual OH-58A accelerometers. This diagnostic system consisted of a Structure-Based Connectionist Network (SBCN) (Ref. 14) which used as its weights the influence coefficients between the gearbox components and accelerometers, and propagated the inputs through its weights to yield as outputs the fault possibility values $p_i \in (0, 1)$ associated with the individual gearbox subsystems (Ref. 15). For quantification purposes, a performance index P_s was obtained for each suite of accelerometers to represent the accuracy of the diagnostic results, as

$$P_s = \sum_{faults} p_i \tag{11}$$

where the summation was carried out over all the available faults that had occurred during the OH-58A experiments. Under ideal conditions and with a perfect accelerometer suite the values of p_i should all be equal to 1 (i.e., the value of P_s should be equal to the number of faults). However, in practice the fault possibility values are smaller than 1 due to imperfect signal conditioning, presence of noise, etc. The analogy used here is that everything else being the same the value of P_s is only affected by the quality of the accelerometer suite when the vibration features from different suites are used as inputs to the diagnostic system. The value of P_s was computed for various accelerometer suites, and then normalized against the largest value of P_s obtained for the same suite size. These normalized P_s values were then used as the basis for ranking the suites. As with the monitoring effectiveness values, the suite with the highest normalized P_s value was assigned to the first category. It should also be noted that in both cases the rankings provide only a relative measure of effectiveness among suites of the same size, and that they should not be perceived as global measures. The normalized P_s values and the associated rankings for suites of 7 accelerometers are included in Table 4 along with the ME values and their corresponding rankings. The results indicate remarkably close agreement between the estimated and empirical rankings, and that except for one mismatch the rankings are identical. Similar analysis was performed for suites of other sizes. A summary of matches and mismatches for all the suites is given in Table 5. The results indicate that out of the 254 possible suites, the estimated rankings of 174 suites match exactly the empirical rankings, 103 mismatch by 1 rank, and 1 suite mismatches by 2 ranks.

Table 4. Rankings obtained from the monitoring effectiveness values and from the diagnostic results for suites of 7 accelerometers. '*' indicates a mismatch between the rankings

Accelerometers included	Monitoring Effectiveness		Empirical	
	ME_s	Rank	P_s	Rank
2,3,4,5,6,7,8	0.983	1	0.888	1
1,3,4,5,6,7,8	0.791	2	0.702	2
1,2,4,5,6,7,8	0.705	2*	0.844	1
1,2,3,5,6,7,8	0.908	1	0.926	1
1,2,3,4,6,7,8	0.200	4	0.200	4
1,2,3,4,5,7,8	0.990	1	1.000	1
1,2,3,4,5,6,8	1.000	1	0.938	1
1,2,3,4,5,6,7	0.940	1	0.843	1

Table 5. Summary comparison of rankings obtained from the monitoring effectiveness values and from the diagnostic results for suites of all sizes

Suites of	Match exactly	Mismatch by		
		1	2	3
7	7	1	0	0
6	17	11	0	0
5	39	17	0	0
4	48	22	0	0
3	38	18	0	0
2	17	11	0	0
1	8	0	0	0
Total	174	80	0	0

The results summarized in Table 5 indicate that the proposed selection method is effective in assessing the monitoring effectiveness of suites of accelerometers. The experimental data set, although one of the most complete sets available in the industry, is not comprehensive enough to render a complete evaluation of the method. The main limitation is the absence of faults in all the components of the gearbox. This could result in an over-estimation of the significance of accelerometers which cover components that failed during the experiments. Similarly, it could lead to devaluation of accelerometers which cover components that did not fail during the experiments. For example, there was only a single fault in Subsystem 2 (mast bearing micropitting), therefore, accelerometer locations that covered this subsystem were given a lower empirical ranking than they actually deserved.

Conclusion

A novel method is introduced for evaluating the significance of accelerometer locations in helicopter gearbox monitoring. This method, which models the structure of the gearbox to define the influence coefficients between components and accelerometers and the overlap of accelerometers in their coverage of components, quantifies the monitoring effectiveness of suites of accelerometer locations. The monitoring effectiveness values are then used as the basis to rank various suites. The application of this selection method is demonstrated to an OH-58A helicopter main gearbox. The results indicate that the rankings provided by this method agree well with empirically obtained rankings. This method, which provides a systematic approach to the selection of accelerometer locations for helicopter gearbox monitoring, addresses a fundamental problem in health and usage monitoring of helicopters.

References

[1]Pratt, J. L., 1986, "Engine and Transmission Monitoring—A Summary of Promising Approaches," *Proceedings of Mechanical Failure Prevention Group 41th Meeting*, October 1986, pp. 229–236.

[2]Astridge, D. G., "Helicopter Transmission-Design for Safety and Reliability," *Proceeding of Institute of Mechanical Engineers*, Vol. 203, 1989, pp. 123–138.

[3]Lyon, R. H., "Structural Diagnostics Using Vibration Transfer Functions," *Sound and Vibration*, January 1995, pp. 28–31.

[4]Smith, J. D., *Gears and their Vibrations*. New York, NY: Marcel Dekker, The Macmillan Press Ltd., 1983.

[5]Lin, H.-H., Huston, R. L., and Coy, J. J., "On Dynamic Loads in Parallel Shaft Transmission: Part I—Modelling and Analysis," *Journal of Mechanisms, Transmission, and Automation in Design*, Vol. 110, June 1988, pp. 221–229.

[6]Boyd, L. S. and Pike, J., "Epicyclic Gear Dynamics," *AIAA Journal*, Vol. 27, No. 5, 1989, pp. 603–609.

[7]Choy, F. K. and Qian, W., "Global Dynamic Modeling of a Transmission System," NASA CR-191117, April 1993.

[8]Mark, W. D., "Use of the Generalized Transmission Error In Equations Of Motion Of Gear Systems," *Journal of Mechanisms, Transmission, and Automation in Design*, Vol. 109, June 1987, pp. 283–291.

[9]Rebbechi, B., Oswald, F. B., and Townsend, D. P., "Dynamic Measurements Of Gear Tooth Friction And Load," NASA TM-103281, October 1991.

[10]Cornell, R. W. and Westervelt, W. W., "Dynamic Tooth Loads And Stressing For High Contact Ratio Spur Gears," *Journal of Mechanical Design*, Vol. 100, 1978, pp. 69–76.

[11]While, M. F., "Rolling Element Bearing Vibration Transfer Characteristics: Effect Of Stiffness," *Journal of Applied Mechanics*, Vol. 46, 1979, pp. 677–684.

[12]Harris, T. A., *Rolling Bearing Analysis*. New York, NY: John Wiley and Sons, Inc., 1966.

[13]Walford, T. L. H. and Stone, B. J., "The Sources Of Damping In Rolling Element Bearings Under Oscillating Conditions," *Proceedings of Institute of Mechanical Engineers*, Vol. 197c, December 1983, pp. 225–232.

[14]Jammu,V. B., Danai, K., and Lewicki, D. G., "Structure-Based Connectionist Network for Fault Diagnosis of Helicopter Gearboxes," *ASME Journal of Mechanical Design*, Vol. 120, No. 1, 1998, pp. 100–105.

[15]Jammu, V. B., Danai, K., and Lewicki, D. G., "Experimental Evaluation of a Structure-Based Connectionist Network for Fault Diagnosis of Helicopter Gearboxes," *ASME Journal of Mechanical Design*, Vol. 120, No. 1, 1998, pp. 106–112.

[16]Kasuba, R. and Evans, J. W., "An Extended Model For Determining Dynamic Loads In Spur Gearing," *Journal of Mechanical Design*, Vol. 103, April 1981, pp. 398–409.

[17]James, M. L., Smith, G. M., Wolford, J. C., and Whaley, P. W., *Vibration of Mechanical and Structural Systems*, Harper Collins College Publishers, New York, NY, 1994.

[18]Zadeh, L. A., "The Concept Of A Linguistic Variable And Its Application To Approximate Reasoning-1," *Information Sciences*, Vol. 8, 1975, pp. 199–249.

[19]Lindsay, R. B., *Mechanical Radiation*. New York, NY: McGraw-Hill Book Company, Inc., 1960.

[20]Lewicki, D. G., Decker, H. J., and Shimski, J. T., "Full-scale Transmission Testing To Evaluate Advanced Lubricants," NASA TM-105668, 1992.